

VSP and Passive Seismic Characterization of Salt Jugs at Well 2A in Hutchinson, Kansas: November 2023 (Part 1*)

Shelby L. Peterie, Julian Ivanov, Marcus Tamburro, Richard D. Miller, Brett C. Bennett, Brett Wedel, Connor Umbrell, Cole Bunker, Carl Gonzales, and Olivia Jones

Kansas Geological Survey
1930 Constant Avenue
Lawrence, KS 66047



Report to

Dale Davis & Spencer Cronin
Burns & McDonnell
9400 Ward Parkway
Kansas City, MO 64114
816-839-9526

Open-file Report 2024-10
March 2024

*Part 1 includes the passive MASW survey and preliminary VSP. Part 2 includes the final VSP.

The Kansas Geological Survey makes no warranty or representation, either express or implied, with regard to the data, documentation, or interpretations or decisions based on the use of this data including the quality, performance, merchantability, or fitness for a particular purpose. Under no circumstances shall the Kansas Geological Survey be liable for damages of any kind, including direct, indirect, special, incidental, punitive, or consequential damages in connection with or arising out of the existence, furnishing, failure to furnish, or use of or inability to use any of the database or documentation whether as a result of contract, negligence, strict liability, or otherwise. This study was conducted in complete compliance with ASTM Guide D7128-05. All data, interpretations, and opinions expressed or implied in this report and associated study are reasonably accurate and in accordance with generally accepted scientific standards.

VSP and Passive Seismic Characterization of Salt Jugs at Well 2A in Hutchinson, Kansas: November 2023 (Part 1)

Executive Summary

This project appraised stress conditions of rock above well 2A dissolution voids by estimating the relative stress field from the calculated shear-wave velocity of the overburden. An estimate of change and potential hazard this stacked void set represents can be obtained by comparing the current stress conditions with those measured on previous surveys. Shear-wave velocities were calculated using passive surface-wave methods where train traffic was used as the energy source. Passive seismic data were acquired along two profiles located on or near well 2A and 4B, which are in proximity to Irsik & Doll elevators in Hutchinson, Kansas.

The multichannel analysis of surface waves (MASW) method provided an estimate of the shear-wave velocity, at a resolution sufficient to loosely map the alluvial/bedrock contact and velocity characteristics of the Permian-aged Shale above the top of the “three finger” dolomite (at approximately 100 meters below ground surface). A key outcome was the differentiation of relative rock stresses based on shear velocity above salt jugs (associated with target wells compared to rock above undisturbed salt or jugs without wide spans of unsupported roof rock (measured on previous full annual surveys) (Peterie et al., 2023). Comparisons of shear-wave velocity profiles over time (time-lapse) provided insights into consistency of overburden stability and therefore indirectly, void dynamics.

Passive MASW data were continuously acquired above wells 2A and 4B, both with a potential to impact surface topography or assets on the Vigindustries and Irsik & Doll sites in Hutchinson, Kansas, over one night (November 16-17, 2023). A continuous sampling approach was used to record all available trains representing valid passive source energy with the goal to maximize opportunities for capturing energy with optimal source orientation and surface-wave characteristics. Surface waves were recorded with frequencies as low as approximately 4.5 hertz (Hz), representing an approximately 60 meter (m) average maximum depth of investigation, which generally represents a depth of more than 40 m below the bedrock surface.

Since shear modulus is the ratio of stress over strain and shear-wave velocity is a function of shear modulus and density, it is possible to estimate relative stress of overburden rocks (shear modulus) from shear-wave velocity values. Local increases in shear-wave velocity above background and without correlation to changes in lithology can be equated to increases in stress associated with changes in the distribution of overburden roof rock loading above dissolution jugs. Relative shear-wave velocity lows may be associated with remnants of a partial or incremental collapse whose vertical movement has been arrested by bulking, or reduction in overburden stress due to changes in the void geometry resulting in stress redistribution within roof rock or changes in rock strength with vertical migration due to different geologic properties related to natural variation.

Well 2A was redrilled in late 2022 to directly investigate possible causes of the consistently observed time-lapse variability. The three largest voids were penetrated in the salt at depths of 125-137, 143-161, and 191-215 m, as well as two other smaller voids. Interaction of the stress fields from these stacked voids could result in complex variations in bedrock stress and therefore shear-wave velocity over time. Three-component, multi-offset and azimuth vertical seismic profile (VSP) data were acquired in well 2A in February 2023 to identify reflecting interfaces and assess potential signals related to voids. Chaotic reflection-like events observed in

the vertical component of the 200' source offset VSP were approximately consistent with expected arrivals times for P-wave diffractions from the tops of three voids encountered during drilling of this well.

Follow-up passive MASW and an offset VSP survey at well 2A were acquired in November 2023 to assess any time-lapse changes in shear-wave velocity and reflection characteristics (and, thus, changes in roof configuration or overburden). The shear wave velocity profiles at lines 10 and 11 are generally consistent with the prior survey in March 2023, suggesting only gradual increase in stress along line 10. Based on cyclic historic observations at well 2A, it is likely another change in the shear modulus will occur at depth followed by a period of relative stability. Given that stress changing events have been incremental with apparent rate of change gradual to date, combined with the observation of the top jug encountered during drilling is at the contact between the base of the Wellington Shale and top of Hutchinson Salt, there is no reason to expect imminent threat of vertical migration at this time.

Results from this second monitoring VSP survey were inconclusive due to a change in surface conditions and therefore source repeatability relative to the baseline survey. Source repeatability is crucial for direct differencing to assess subtle changes in roof configuration (or lack thereof). Therefore, VSP data will be recollected in the near future using the source location established during the baseline survey to optimize repeatability for differencing and will represent Part 2 of this report.

Introduction

Material properties (specifically stress accumulations) measured as a function of depth above abandoned salt jugs in Hutchinson, Kansas, appear related to the load density associated with the tensional dome of these jugs. Localized escalation in stress (as indicated by increased shear-wave velocity) above subterranean voids is one indicator of an increased potential for roof failure and void migration (Eberhart-Phillips et al., 1989; Dvorkin et al., 1996; Khaksar et al., 1999; Sayers, 2004). Previous studies, using both active and passive seismic wavefield characteristics, suggest perturbations in the shear-wave velocity field immediately above voids can be correlated to characteristics of the unsupported roof spans of salt jugs in the Hutchinson area (Sloan et al., 2010).

The strength of individual rock layers can be qualitatively described in terms of stiffness/rigidity and empirically estimated from relative comparisons of time-lapse shear-wave velocity measurements. Shear-wave velocity is directly proportional to stress and inversely related to non-elastic strain. Since the shear-wave velocity of earth materials changes when stress and any associated elastic strain on those materials becomes “large” (nonelastic), it is reasonable to suggest load-bearing roof rock above mines or dissolution voids may experience elevated shear-wave velocities due to excessive loading between pillars or, in the case of voids, loading between supporting side walls. This localized increase in shear velocity is not related to increased strength but to increased load as defined by Young’s Modulus. High-velocity shear-wave encompassing low-velocity anomalies (“halo” anomalies) are suggested to be key indicators of near-term roof failure. All these phenomena have been observed within the overburden above voids in the Hutchinson Salt Member in Hutchinson at depths greater than 30 m below the bedrock surface.

Previous research projects at several selected locations on Vigindustries’ legacy solution mining property in Hutchinson, Kansas, correlated measured shear-wave velocities with the condition of dissolution void roofs and the related physical properties of the overburden. In 2008, active seismic reflection imaging was used to evaluate the effectiveness of using the

calculated shear-wave velocity as a relative measure of local stress above voids consistent in the size and depth as those prevalent at the Vigindustries site. It was determined that the integrity/consistency of the overlying strata could be reasonably estimated using shear-wave seismic reflection imaging. The lack of necessary ultra-low-frequency surface waves in the recorded wavefield negated attempts to use active-source multi-channel analysis of surface waves (MASW) to estimate shear velocity in the lithified rocks above the voids and near the top of bedrock (Miller et al., 2009).

Uncontrolled local industrial and transportation activities represent sound energy sources that can produce the necessary low frequency seismic waves to interrogated rock material at depths greater than 60 m using passive methods (Miller, 2011). A key attribute of this method is the ability to estimate shear-wave velocities using MASW to depths more than double those possible using standard active sources (Park et al., 2004). Results of passive MASW studies at and near this site suggest that this method is effective in identifying known jugs with heightened risk for upward migration (Miller, 2011; Ivanov et al., 2013).

Following the active seismic imaging study in 2008, two-dimensional (2-D) passive MASW surveys have been acquired at the Hutchinson Mosaic site since 2012 to appraise the stability/consistency of overburden at selected wells (Table 1). Results of these investigations suggested a normal stress regime with natural geologic variation is present above most wells with known jugs. Shear velocity calculations above a few wells were noted to be outside what might be considered normal for the area and justified more attention. Individually, each profile represents a snapshot in time; however, when combined with previous observations at the same locations, time-lapse analysis can be used to monitor for temporal variation in shear velocity, which could be an indication of relative void stability and dynamics.

Vertical seismic profiling (VSP) is a downhole technique used for determining compressional wave (P-wave, V_p) and shear wave (S-wave, V_s) velocities and mapping reflecting interfaces (contact between materials with different physical properties) and relating those to geologic structures in close proximity to a borehole (Hardage, 1985a; Stewart and DiSiena, 1989). For a traditional VSP, the source is located near the borehole and provides a measure of seismic properties and images very near (an offset distance that is a small fraction of depth to deepest borehole sampling point) to the well. For an offset VSP, the source is located at various offset distances from the borehole with the most distant source locations equal to the depth to the deepest sensor location. Well 2A was redrilled in late 2022 and three-component (3-C) multi-offset VSP data were acquired shortly after completion of the well to identify reflecting interfaces and assess anomalous signal that may be related to voids associated with these wells. Depending on source repeatability, direct differencing from time-lapse surveys can be used to image changes related to void growth, changes in shear modulus, or changes in the roof configuration.

Table 1. Dates of wells evaluated during 2-D passive MASW surveys at the Carey Boulevard Research Area (CBRA).

Date	Wells
August 2012	2A, 1B, 2B, 3B, 5B, 6B, 7B, 12B
October 2012	2B, 4B, 6B, 17, 45, 52, 53, 59
March 2013	2A, 4B
November 2014	2A, 3B, 4B
March 2015	1B, 2B, 3B, 6B, 8A, 8B, 10B, 11B, 12B, 13B, 14B, 15B, 17, 18, 22A, 23, 23B, 29, 30, 39, 41, 42, 44, 45, 46, 86, 87, 88, 89, 90, 92
May 2015	2A, 4B
June 2015	4A, 6B, 7A, 7B, 52, 53, 59, 60
November 2017	2A, 4A, 7A, 8A, 1B, 2B, 3B, 4B, 6B, 7B, 8B, 10B, 11B, 12B, 13B, 14B, 15B, 17, 18, 22A, 23, 23B, 29, 30, 39, 41, 42, 44, 45, 46, 52, 53, 59, 60, 86, 87, 88, 89, 90, 92
October 2018	2A, 4B
December 2018	1B, 2B, 3B, 4A, 4B, 6B, 7A, 7B, 8A, 8B, 10B, 11B, 12B, 13B, 14B, 15B, 17, 18, 22A, 23B, 23, 29, 30, 39, 41, 42, 44, 45, 46, 52, 53, 59, 60, 86, 87, 88, 89, 90
December 2019	1B, 2A, 2B, 3B, 4A, 4B, 5B, 6B, 7A, 7B, 8A, 8B, 10B, 11B, 12B, 13B, 14B, 15B, 17, 18, 22A, 23B, 23, 29, 30, 39, 42, 44, 45, 46, 52, 53, 59, 60, 88, 89, 90, 92
August 2020	2A, 4A, 7A, 15B, 59
November 2020	1B, 2A, 2B, 3B, 4A, 4B, 5B, 6B, 7A, 7B, 8A, 8B, 10B, 11B, 12B, 13B, 14B, 15B, 17, 18, 22A, 23B, 23, 29, 30, 39, 42, 44, 45, 46, 52, 53, 59, 60, 88, 89, 90, 92
November 2021	1B, 2A, 2B, 3B, 4A, 4B, 5B, 6B, 7A, 7B, 8A, 8B, 10B, 11B, 12B, 13B, 14B, 15B, 17, 18, 19, 20, 22A, 23B, 23, 25, 26, 29, 30, 33, 36, 39, 41, 42, 44, 45, 46, 52, 53, 59, 60, 88, 89, 90, 92, 94
March 2023	1B, 2A, 2B, 3B, 4A, 4B, 5B, 6B, 7A, 7B, 8A, 8B, 10B, 11B, 12B, 13B, 14B, 15B, 17, 18, 19, 20, 22A, 23B, 23, 25, 26, 29, 30, 33, 36, 39, 41, 42, 44, 45, 46, 52, 53, 59, 60, 88, 89, 90, 92, 94
November 2023	2A, 4B

Geologic and Geophysical Setting

The Permian-aged Hutchinson Salt Member occurs in central Kansas, northwestern Oklahoma, and the northeastern portion of the Texas panhandle and is prone to and has an extensive history of dissolution and formation of sinkholes (Figure 1). In Kansas, the Hutchinson Salt Member possesses an average net thickness of 75 m and reaches a maximum of more than 150 m in the southern part of the basin. Deposition occurring during fluctuating sea levels caused numerous halite beds, 0.2 to 3 m thick, to be formed interbedded with shale, minor anhydrite, and dolomite/magnesite. Individual salt beds may be continuous for only a few miles despite the remarkable lateral continuity of the salt as a whole (Walters, 1978).

The distribution and stratigraphy of the salt is well documented (Dellwig, 1963; Holdoway, 1978; Kulstad, 1959; Merriam, 1963). The salt reaches a maximum thickness in central Oklahoma and thins to depositional edges on the north and west, erosional subcrop on the east, and facies changes on the south. The increasing thickness toward the center of the salt bed is due to a combination of increased salt and more and thicker interbedded anhydrites. The Stone Corral Formation (a well-documented seismic marker bed) overlies the salt throughout

Kansas (McGuire and Miller, 1989). Directly above the salt at this site is a thick sequence of Permian shale capped with a saturated interval of Pliocene-Pleistocene sediments.

The upper approximate 76 m of rock immediately below around 21 m of Pliocene-Pleistocene sediments at this site is a Permian shale sequence (Merriam, 1963). The Chase Group (top at 300 m deep), lower Wellington Shale (top at approximately 245 m deep), Hutchinson Salt (top at near 120 m deep), upper Wellington Shale (top at around 75 m deep), and Ninnescah Shale (top at approximately 25 m deep) make up the Permian portion of the section

(Figure 2). Bedrock is defined as the top of the Ninnescah Shale with the unconsolidated Pliocene-Pleistocene Equus beds making up the majority of the approximate upper 21 m of sediment. The thickness of Quaternary alluvium that fills the stream valleys and paleosubsidence features extends from 0 to as much as 90 m, depending on the dimensions of the features.

Recent dissolution of the salt and resulting subsidence of overlying sediments forming sinkholes has generally been associated with mining or saltwater disposal (Walters, 1978). Historically, these sinkholes can manifest themselves as a risk to surface infrastructure. The rate of surface subsidence can range from gradual to very rapid. Besides risks to surface structures, subsidence features potentially jeopardize the natural segregation of groundwater aquifers, greatly increasing their potential to negatively impact the environment (Whittemore, 1989, 1990). Natural sinkholes resulting from dissolution of the salt by localized leaching within natural flow systems that have been altered by structural features (such as faults and fractures) are not uncommon west of the main dissolution edge (Merriam and Mann, 1957).

Caprock and its characteristics are a very important component of any discussion concerning dissolution, subsidence, and formation of sinkholes. The Permian shales (Wellington and Ninnescah) that overlay the Hutchinson Salt Member are highly variable and can range from less than 60 m to more than 100 m thick in this area and are characterized as generally unstable when exposed to freshwater, being susceptible to sloughing and collapse (Swineford, 1955). These Permian shales tend to be red or reddish-brown and are commonly referred to as “red beds.” Permian red beds are extremely impermeable to water and have provided an excellent seal between the freshwaters of the Equus beds and the extremely water-soluble Hutchinson Salt Member. The modern-day

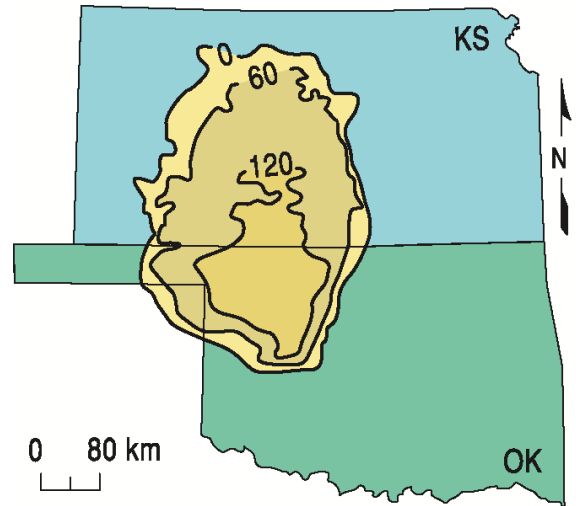


Figure 1. Approximate extent of salt formation, with contour intervals expressed in meters.

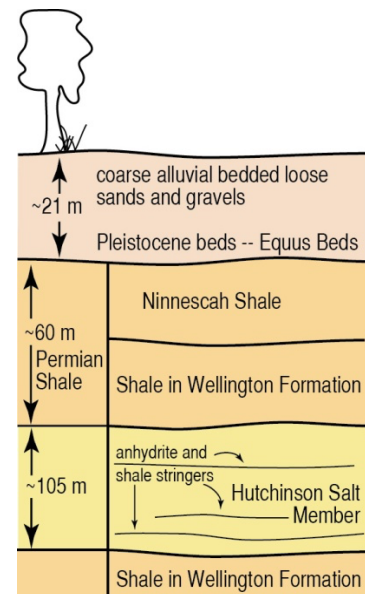


Figure 2. Generalized geology with approximate depths

expanse and mere presence of the Hutchinson Salt is due to the protection from freshwater provided by these red beds.

Isolating the basal contact of the Upper Wellington Formation shales provides key insights into the general strength of roof rock expected if dissolution-mined salt jugs (cavities or voids in the salt that form after salt has been dissolution mined in proximity to the wells) reach the top of the salt zone. Directly above the salt/shale contact is approximately 6 m thick dark-colored shale with joint and bedding cracks filled with red halite (Walters, 1978). Once unsaturated brine comes in contact with this shale layer, these red halite-filled joints and bedding planes are rapidly leached, leaving an extremely structurally weak layer.

Field Layout and Data Acquisition

Offset VSP data was collected at well 2A on November 16, 2023. Multipurpose rubber coating was applied to the exterior housing of the downhole tool and weather stripping was applied to the band to improve coupling and reduce mechanical oscillations. The vertical source was a 16 lb sledgehammer impacting a steel plate. The source location was 60 m west of well 2A in the hardpack parking area. The source location for the previously acquired VSP was in the grassy area due west and slightly south of well 2A. It was moved to the parking area just north of the road to avoid interfering with truck traffic at the grain elevator. The downhole receiver was a three-component (3-C) Geostuff BHG-2 geophone with steel band clamping mechanism. The receiver was lowered and clamped to the casing wall at 3 m intervals down to a maximum depth of 112 m. A minimum of three consecutive shots were acquired at each depth and vertically stacked to assure strong signal. Findings from the VSP survey will be provided in Part 2 of this report.

Following the downhole survey, a passive survey was conducted along two lines intersecting wells 2A and 4B, coincident with lines collected each year during the annual monitoring survey. To ensure the highest quality [e.g., signal-to-noise ratio (S/N)] data and maximum crew safety, receivers were deployed during daylight hours and train data were recorded at night when cultural and industrial noise was minimal, thereby providing the highest possible S/N. Analysis of previous seismic energy sources captured during passive recording at this site clearly indicated trains at distances of 2 kilometers (km) or more provided the best broad spectrum, low-frequency seismic energy (Miller, 2011). Since seismic energy with characteristics best suited for this study may arrive when trains are at distances greater than can be detected by spotters, seismic energy was recorded continuously throughout the night to ensure the capture of optimum data.

Passive data were acquired November 16-17, 2023. Two seismic lines (Figure 3) were deployed during the day of November 16th. Line layout was designed to cross directly over wells 2A and 4B. A 2-D square grid of receivers was also deployed and recorded simultaneously to allow determination of the incident orientation of passive seismic energy. This 2-D monitoring/alignment grid consisted of 128 receivers spaced at 5 m intervals, configured to form four concentric expanding squares with 10, 30, 50, and 70 m sides (Figure 4). Seismic receivers were single ION 4.5 Hz geophones spaced at 3 m intervals along the lines. The seismic lines collectively totaled approximately 140 m in length. Data were recorded with a 400+ channel 24-bit Geometrics Geode distributed seismic system. Seismic records from the Geometrics system were 30 seconds (s) long with a 2 millisecond (ms) sampling interval. In total, 797 seismic records were recorded over the night of November 16.

Processing and Analysis

Passive data were processed using algorithms and software developed at the Kansas Geological Survey (KGS). The passive method used for this study is well published and has consistently proven effective for producing good-quality results on other studies (Park et al., 2004; Ivanov et al., 2013). The continuous-data-acquisition method records energy from nearby sources at various orientations with respect to the seismic line. Data from the 2-D grid are evaluated for optimized source alignment with respect to each 1-D seismic line allowing data rotation and analysis or direct analysis of only data from near in-line sources.

For each line, the surface-wave amplitudes recorded by the 2-D grid were plotted as phase velocity versus frequency across a range of azimuths (0 to 360 degrees) (Figure 5), relative to the seismic line. This display was effective for identifying the best broad-band, low-frequency source energy with an azimuth as near zero as possible. Seismograms for each line were selected and segmented into the shortest groups of receivers (“spread length”) with optimum source characteristics that resulted in good quality dispersion patterns on phase velocity versus frequency plots (Figure 6). Additionally, the quality of the dispersion curves was based on the greatest percentage of high-amplitude fundamental-mode Rayleigh-wave energy and minimal higher-order surface-wave interference.

Fundamental mode dispersion curves were picked and inverted to obtain a 2-D section of shear-wave velocity as a function of depth. The apparent velocity (v_{app}) is:

$$v_{app} = \frac{v_{act}}{(\cos \theta)} \quad (\text{Equation 1})$$

where v_{act} is the actual seismic velocity and θ is the azimuth of the source with respect to the seismic line determined from the azimuth versus frequency plot. Thus, the percent increase in velocity (Δv) is:

$$\Delta v = \frac{1}{\cos \theta} - 1 \quad (\text{Equation 2})$$

Equation 2 was used to calculate the increase in velocity due to the source azimuth for each line (Table 2).

Table 2. Directions of the passive seismic sources and the seismic lines; spread length used for processing, the angle of the source with respect to the line (θ , in degrees counterclockwise from east), and velocity correction applied to correct for apparent velocity (Δv) of oblique source orientations.

	processing spread length(s)	source orientation	line orientation	θ	Δv
Line 10	81 m	180°	180°	0°	0%
Line 11	81 m	110°	74°	36°	23.6%

Downhole data were processed with conventional VSP techniques (Hardage, 1985b) using SeisUtilities software developed at the KGS. Consecutive shots at each station were vertically stacked to maximize S/N. The first breaks of compressional-waves (P-waves) were

picked on vertical-component traces. Frequency-wavenumber ($f-k$) and bandpass filters were applied to attenuate down-going waves and enhance reflected signal, respectively. Finally, static corrections based on picked first arrival times were applied to flatten reflections. Follow-up VSP survey data will be presented with the November 2023 and February 2023 data and findings in Part 2 of this report.

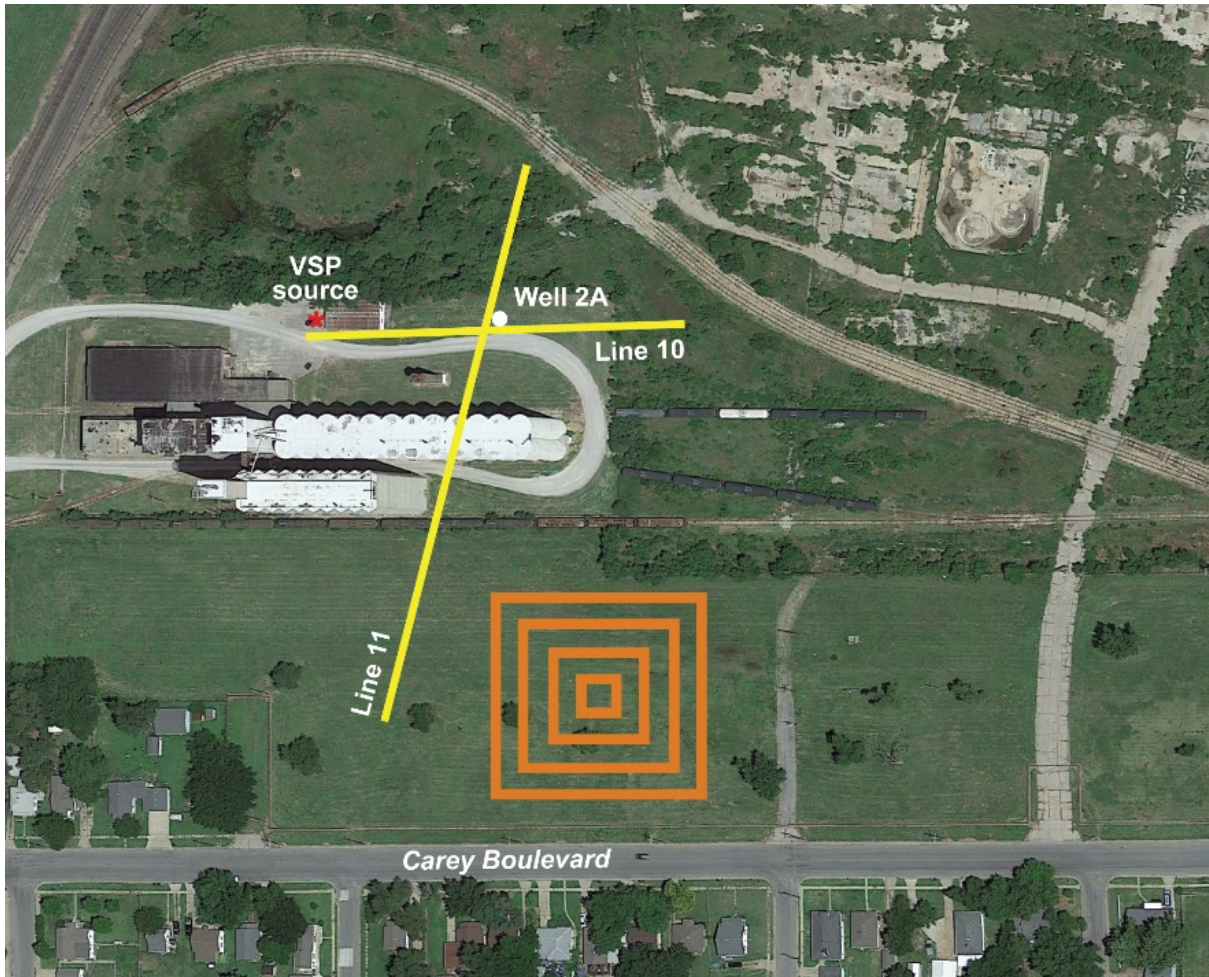


Figure 3. Aerial photo with GPS locations of passive seismic lines (yellow) crossing well 2A, 2-D grid of receivers (orange), and VSP source location (red) in the November 2023 study.

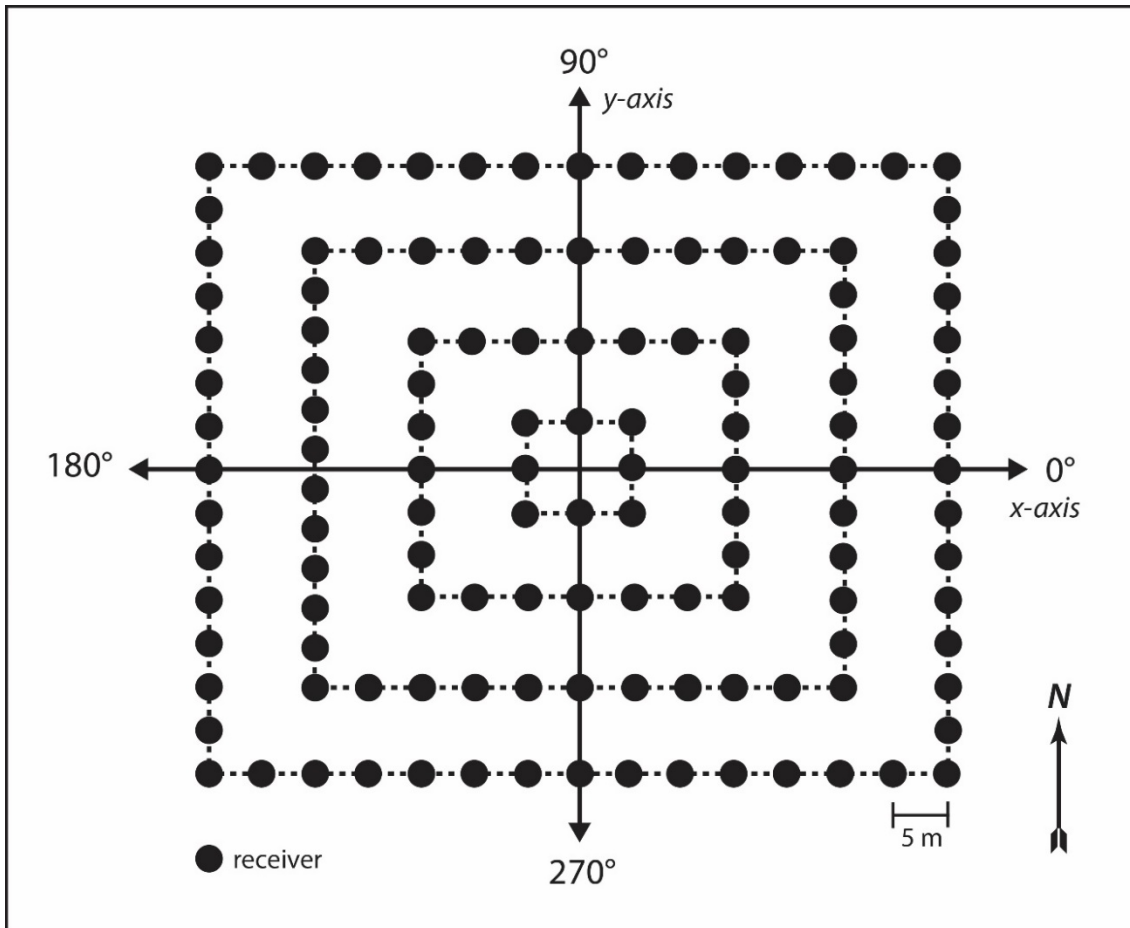


Figure 4. Four nested square arrays were deployed to construct the 2-D square grid for determining incident source azimuth information.

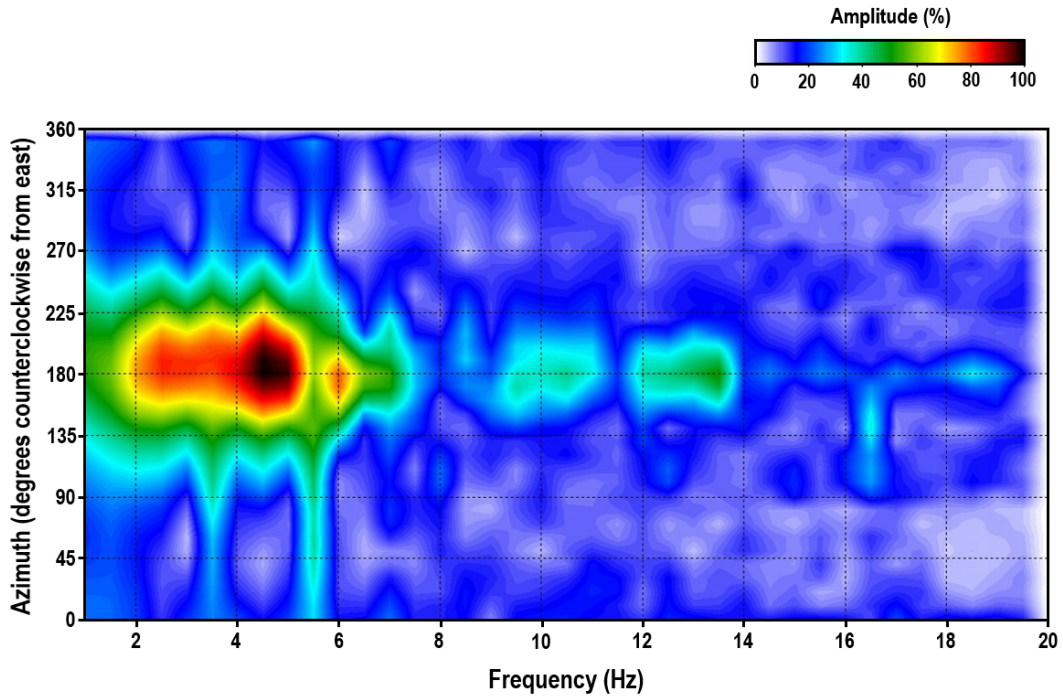


Figure 5. Azimuth plot indicating the direction of the dominant passive source energy (in degrees counterclockwise from east). Here, the dominant passive source energy is centered on approximately 180°.

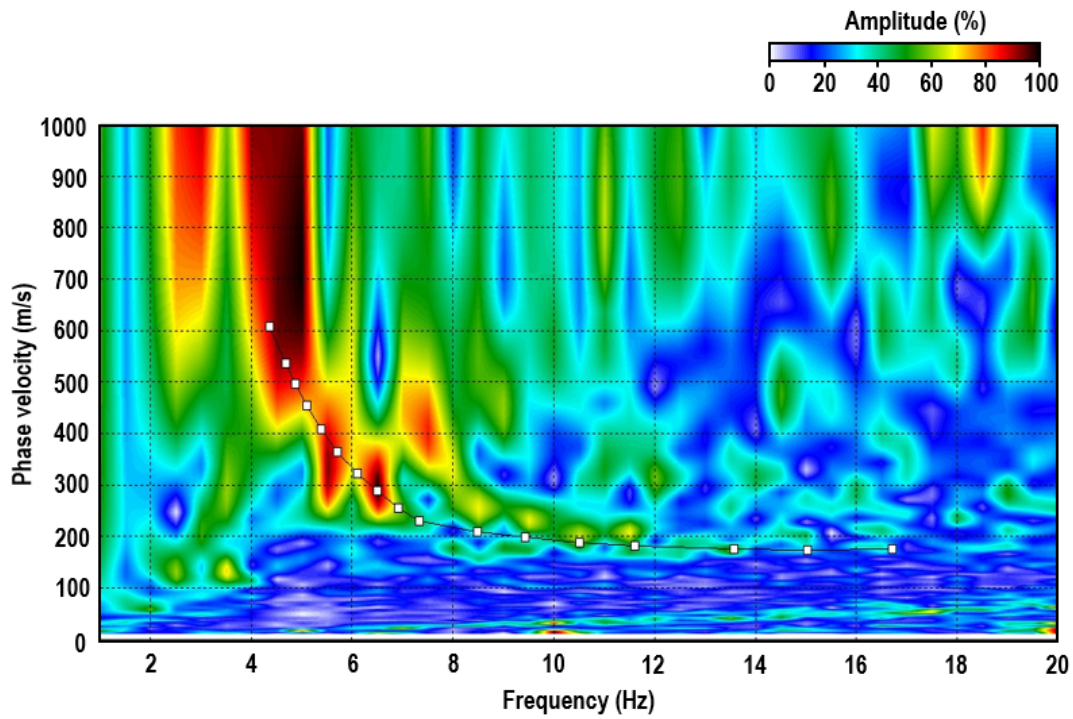


Figure 6. Dispersion pattern with high signal-to-noise ratio of the fundamental-mode Rayleigh wave.

Field Results and Observations

MASW: General Trends

The average velocity of the upper 15 m is approximately 175 m/s, consistent with the unconsolidated/alluvial sediment expected in this area and with the downhole data acquired in well 15B in January 2023. The velocity gradient at 15 m coincides with the interface between the unconsolidated sediment and shale bedrock. Average depth of investigation was 50-60 m across all lines as a result of surface wave frequencies generally above 4 Hz—lower frequencies would have resulted in deeper sampling depths. Dispersion curves were obtained using different spread lengths for each line. These changes in spread lengths were to avoid distortion in the surface wave dispersion patterns at low frequencies. Using the shortest optimal spread length on each line resulted in high lateral resolution and spatial extent of the resulting 2-D profiles while maintaining dispersion patterns at lower frequencies.

Line 10

Line 10 is a W-E oriented line that crosses well 2A at station 1022.5 (Figure 7). The westernmost 5 geophones are located on the road used to access the grain elevator and utilized rock plates instead of steel spikes. Time-lapse changes observed at well 2A since 2013 suggest periods of elevated stress/velocity, with subsequent reduced shear velocity indicative of a drop in overburden strength, separated by periods of relative stability (see Figure A-1 in the appendix). Between the May 2015 and November 2017 surveys, velocity in the overburden at well 2A increased slightly (~15%) but was consistent with the native bedrock velocity range. This suggests the void at that time was in a state of relative stability with only minor changes in stress with void stabilization. Multiple mode behavior was noted west of well 2A in 2020 suggesting heterogeneity at deeper depths where multiple stress states may have existed within the shale bedrock, and a period of relative stability in 2021. Overall, the bulk-velocity in November 2023 is similar to but slightly higher than 2021 and March 2023, with the most notable increase at and east of well 2A.

Line 11

Line 11 is oriented N-S over well 2A at station 1124 and well 4B at station 1151 (Figure 8). Line 11 had a 20% decrease in velocities centered on well 2A and 15% decrease between well 2A and 4B in 2015 (see Figure A-1 in the appendix). Beginning in 2017, velocity was slightly higher and more consistent across the line and appeared to remain stable. In 2020, the velocities around well 2A decreased in comparison to 2019, suggesting a failure and redistribution of stress may have occurred. A corresponding decrease in velocity was not observed on the nearly perpendicular line 10. Therefore, velocity variation was azimuthal, which may be associated with changes in material strength in different directions from the well head. Fracture orientations are often consistent with the direction of slowness. In March and November of 2023, velocities on lines 10 and 11 are similar to 2020, suggesting consistency in the azimuthal anisotropy and interpreted changes in material strength.

Well 2A VSP

The first time-lapse VSP at well 2A (Figure 9, bottom) acquired in November 2023 has a relatively low S/N. The general features are similar to the February 2023 VSP with relatively chaotic reflection- or diffraction-like events (Figure 9c, bottom). The same prominent events from February are identifiable in November (see highlighting in Figure 9), but at a lower S/N.

The most effective time-lapse surveys require consistent source energy and receiver coupling to allow meaningful and confident quantitative differencing necessary for monitoring subtle subsurface changes. Coupling between the downhole tool and borehole should be extremely similar between the February and November surveys. However, due to the change in source location necessary to safely avoid vehicle traffic, surface conditions at the different source locations significantly impacted source coupling and energy characteristics, resulting in reduced signal amplitude relative to noise in the November survey. After detailed analysis, it is most likely the observed differences in the VSP wavefield arrival characteristics are due to changes in source coupling and associated seismic energy. Therefore, differencing of these two data sets would produce results that would not represent true changes in the subsurface. For that reason, a repeat VSP will be acquired in well 2A during the next annual monitoring survey with the source location coincident with the location used during the February 2023 survey.

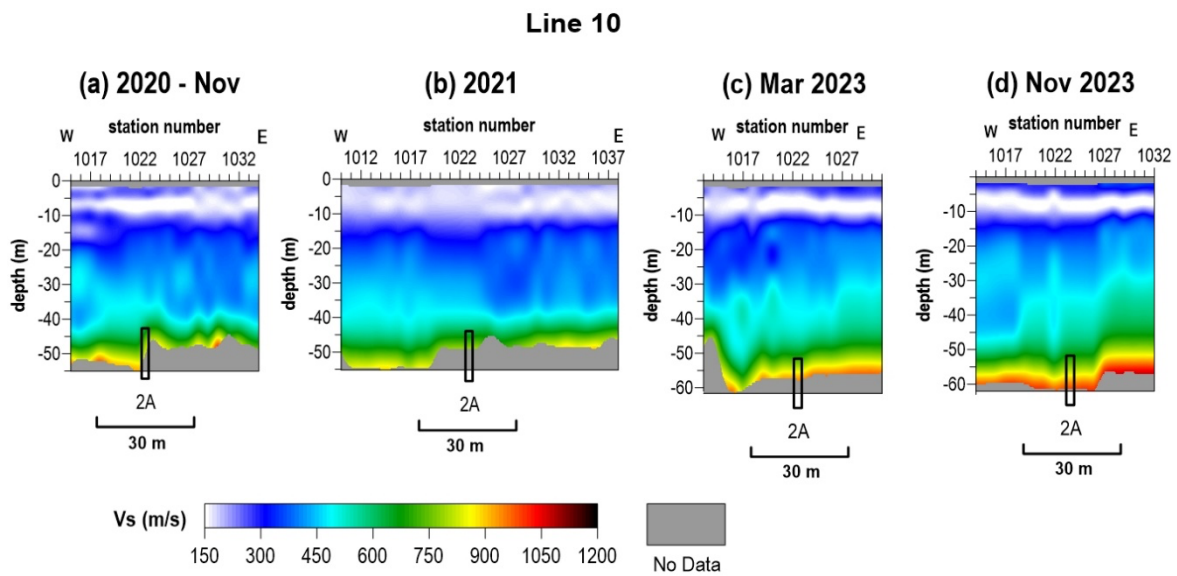


Figure 7. Shear-wave velocity profiles from line 10 from (a) November 2020, (b) November 2021, (c) March 2023 and (d) November 2023.

Line 11

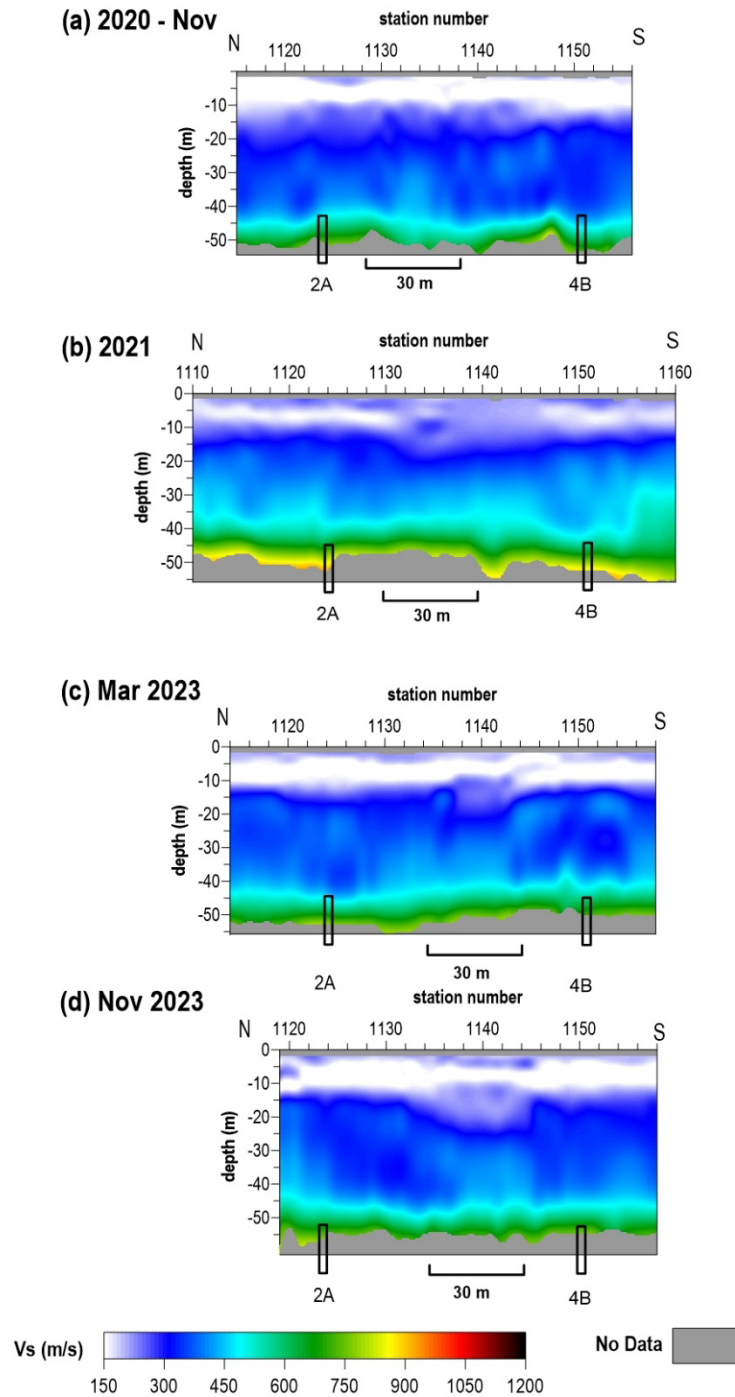
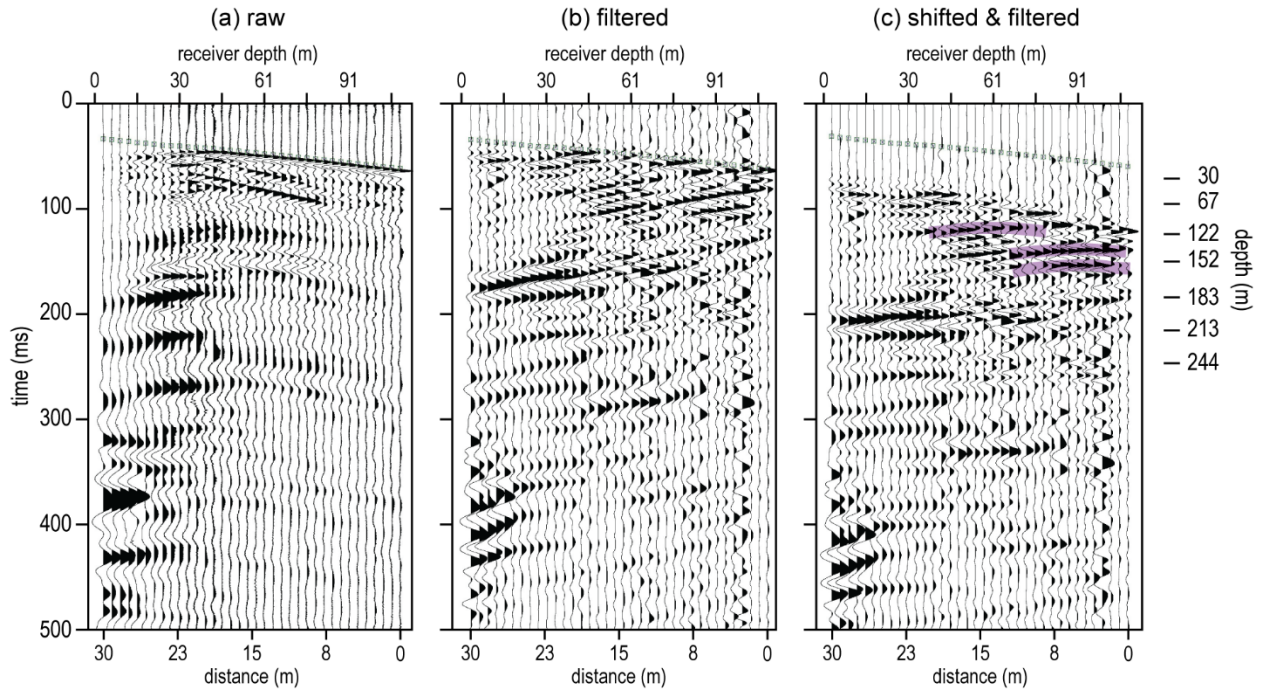


Figure 8. Shear-wave velocity profiles from line 11 from (a) November 2020, (b) November 2021, (c) March 2023, and (d) November 2023 investigation with approximate locations of well 2A and well 4B.

February 2023



November 2023

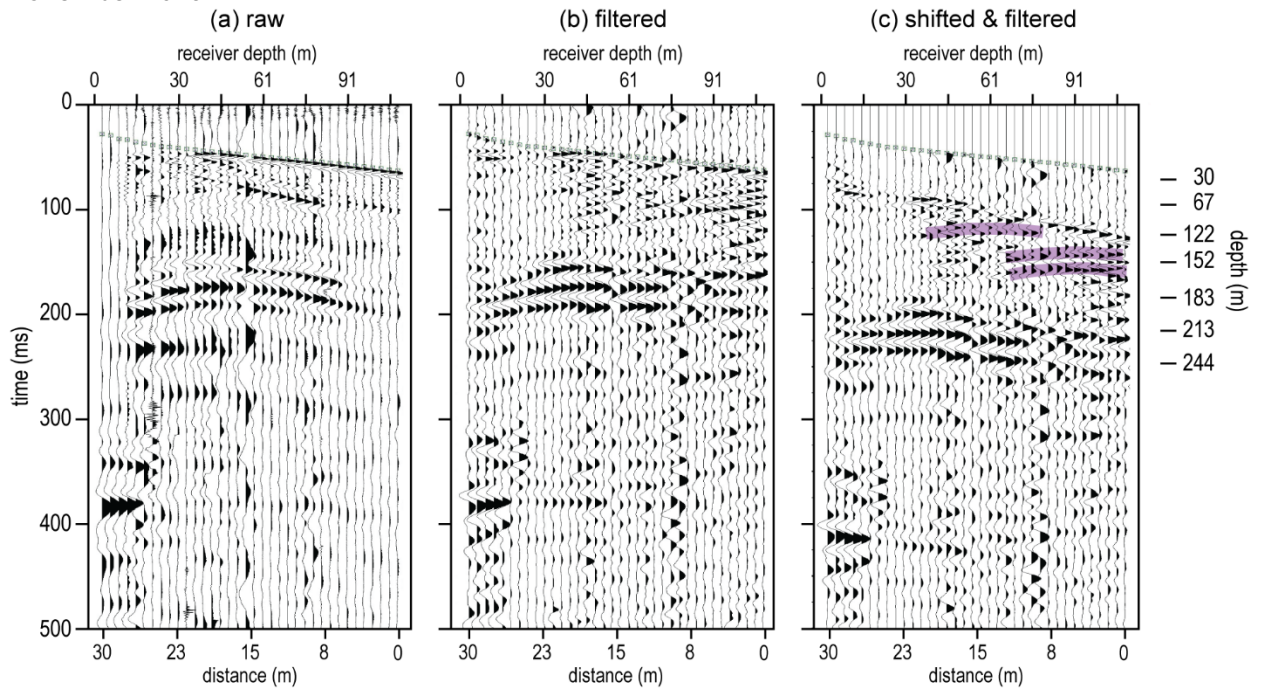


Figure 9. Downhole profiles from the VSP survey on well 2A in *(top)* February and *(bottom)* November 2023.

Interpretation, Conclusions and Recommendations

Overall, very little change was observed in the shear wave velocity profiles acquired along lines 10 and 11 between March and November 2023. Slightly increased velocity observed on line 10 is consistent with gradually increasing stress. Similar to previous years, azimuthal velocity anisotropy suggests reduced strength in the north-south direction and/or unequal loading and distribution of stress, possibly indicative of fracture orientations. Based on the cyclic nature of historic observations at well 2A, this slight increase is likely the precursor to another incremental failure at depth within the salt with a redistribution and alleviation of this very small build up in stress along line 10, thereby equalizing velocities between lines 10 and 11, which will be followed by an upcoming period of relative stability. Given that failure has been incremental and gradual to date (with no evidence of significant vertical migration from drilling results), **there is no reason to expect imminent threat of significant vertical migration at this time.**

Surface conditions at the new source location for the follow up VSP survey proved to be detrimental to S/N of void signatures and prohibited time-lapse differencing intended to highlight subtle changes in roof configuration or void growth. VSP results from the November survey were therefore inconclusive. Source repeatability is crucial for direct differencing to assess changes in roof configuration (or lack thereof). A follow-up survey will be completed around the time of the annual monitoring survey during Spring 2024 at a time when cables crossing the road on the north side of the grain elevator will not interfere with truck traffic or elevator operations. Consistency in source location and associated surface conditions should improve source repeatability and wavefield characteristics between the February 2023 and March/April 2024 surveys, allowing for optimal time-lapse differencing. Findings from the VSP survey will be provided as Part 2 of this report upon completion of a repeat VSP survey of well 2A.

References

- Dellwig, L.F., 1963, Environment and mechanics of deposition of the Permian Hutchinson Salt Member of the Wellington shale: Symposium on Salt, Northern Ohio Geological Society, p. 74-85.
- Dvorkin, J., A. Nur, and C. Chaika, 1996, Stress sensitivity of sandstones: *Geophysics*, v. 61, p. 444-455.
- Eberhart-Phillips, D., D.-H. Han, and M.D. Zoback, 1989, Empirical relationships among seismic velocity, effective pressure, porosity, and clay content in sandstone: *Geophysics*, v. 54, p. 82-89.
- Hardage, B.A., 1985a, Vertical Seismic Profiling: The Leading Edge, 4, 11, 59-60, <https://doi.org/10.1190/1.1487141>.
- Hardage, B.A., 1985b, Vertical Seismic Profiling, Part A: Principles. *Geophysical Press*, 450 p.
- Holdaway, K.A., 1978, Deposition of evaporites and red beds of the Nippewalla Group, Permian, western Kansas: Kansas Geological Survey Bulletin 215.
- Ivanov, J., R.D. Miller, S.L. Peterie, J.T. Schwenk, J.J. Nolan, B. Bennett, B. Wedel, J. Anderson, J. Chandler, and S. Green, 2013, Enhanced passive seismic characterization of high priority salt jugs in Hutchinson, Kansas: Preliminary report to Burns & McDonnell Engineering Company.
- Khaksar, A., C.M. Griffiths, and C. McCann, 1999, Compressional- and shear-wave velocities as a function of confining stress in dry sandstones: *Geophysical Prospecting*, v. 47, p. 487-508.
- Kulstad, R.O., 1959, Thickness and salt percentage of the Hutchinson salt; in Symposium on Geophysics in Kansas: Kansas Geological Survey Bulletin 137, p. 241-247.
- McGuire, D., and B. Miller, 1989, The utility of single-point seismic data; in Geophysics in Kansas, D.W. Steeples, ed.: Kansas Geological Survey Bulletin 226, p. 1-8.
- Merriam, D.F., 1963, The Geologic History of Kansas: Kansas Geological Survey Bulletin 162, 317 p.
- Merriam, D.F., and C.J. Mann, 1957, Sinkholes and related geologic features in Kansas: *Transactions of the Kansas Academy of Science*, v. 60, p. 207-243.
- Miller, R.D., 2011, Progress report: 3-D passive surface-wave investigation of solution mining voids in Hutchinson, Kansas: Interim report to Burns & McDonnell Engineering Company, January, 9 p.
- Miller, R.D., J. Ivanov, S.D. Sloan, S.L. Walters, B. Leitner, A. Rech, B.A. Wedel, A.R. Wedel, J.M. Anderson, O.M. Metheny, and J.C. Schwarzer, 2009, Shear-wave study above Vigindustries, Inc. legacy salt jugs in Hutchinson, Kansas: Kansas Geological Survey Open-file Report 2009-3.
- Park, C., R. Miller, D. Laflen, N. Cabrillo, J. Ivanov, B. Bennett, and R. Huggins, 2004, Imaging dispersion curves of passive surface waves [Exp. Abs.]: Annual Meeting of the Soc. of Expl. Geophys., Denver, Colorado, October 10-15, p. 1357-1360.
- Peterie, S.L., J. Ivanov, M. Tamburro, R.D. Miller, B.C. Bennett, B. Wedel, C. Umbrell, C. Bunker, C. Gonzales, and O. Jones, 2023, Passive Seismic Characterization of High Priority Salt Jugs in Hutchinson, Kansas: March 2023: Report to Burns & McDonnell Engineering Company.
- Sayers, C.M., 2004, Monitoring production-induced stress changes using seismic waves [Exp. Abs.]: Annual Meeting of the Soc. of Expl. Geophys., Denver, Colorado, October 10-15, p. 2287-2290.
- Sloan, S.D., S.L. Peterie, J. Ivanov, R.D. Miller, and J.R. McKenna, 2010, Void detection using near-surface seismic methods; in Advances in Near-Surface Seismology and Ground-Penetrating Radar, SEG Geophysical Developments Series No. 15, R.D. Miller, J.D. Bradford, and K. Holliger, eds.: Tulsa, Society of Exploration Geophysicists, p. 201-218.
- Stewart, R.R., and J.P. DiSiena, 1989, The values of VSP in interpretation: *The Leading Edge*, 8, 12, 16-23, <https://doi.org/10.1190/1.1439597>.
- Swineford, A., 1955, Petrography of upper Permian rocks in south-central Kansas: State Geological Survey of Kansas Bulletin 111, 179 p.
- Walters, R.F., 1978, Land subsidence in central Kansas related to salt dissolution: Kansas Geological Survey Bulletin 214, 82 p.
- Whittemore, D.O., 1989, Geochemical characterization of saltwater contamination in the Macksville sink and adjacent aquifer: Kansas Geological Survey Open-file Report 89-35.
- Whittemore, D.O., 1990, Geochemical identification of saltwater contamination at the Siefkes subsidence site: Report for the Kansas Corporation Commission.

Appendix

Line 10

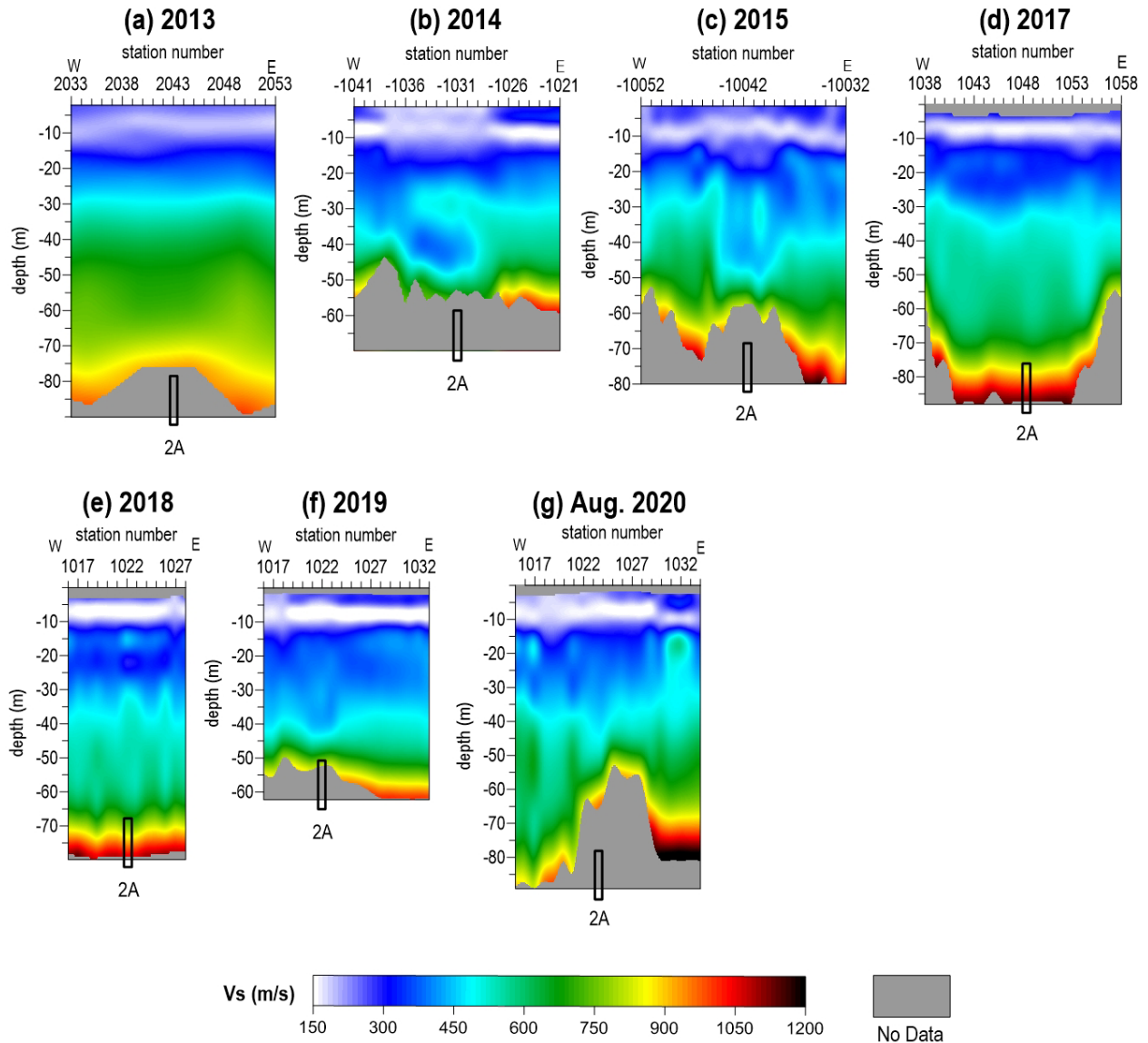


Figure A-1. Shear wave velocity profiles for line 10 over well 2A for 2013-August 2020.

Line 11

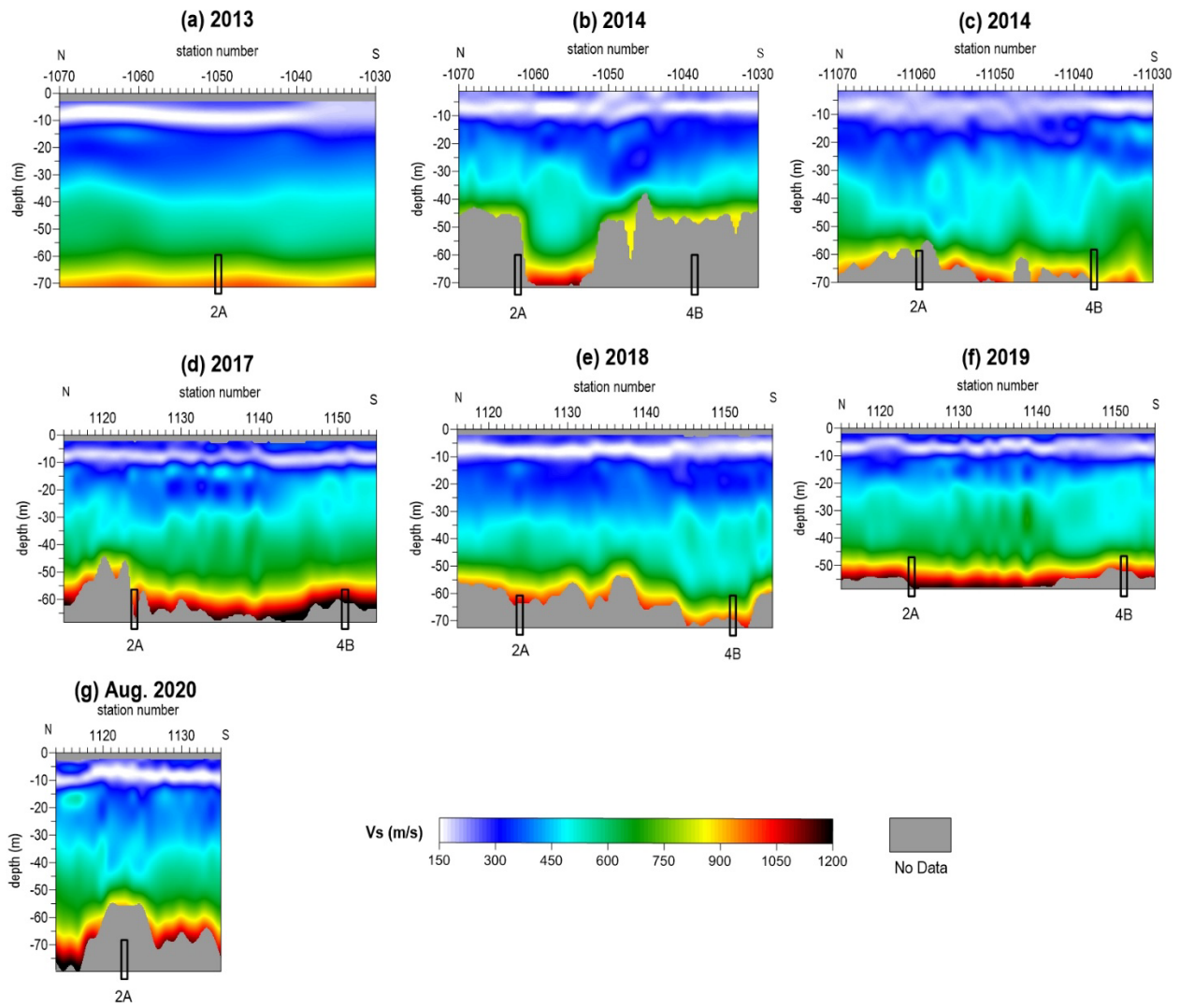


Figure A-2. Shear wave velocity profiles for line 11 over well 2A for 2013-August 2020.